Analytical solution for switched band matching networks

Norouzian, F.; Gardner, P.

DOI:
10.1049/ic.2012.0063

Document Version
Peer reviewed version

Citation for published version (Harvard):
Norouzian, F & Gardner, P 2012, Analytical solution for switched band matching networks. in *IET Seminar Digest.* vol. 2012, pp. 43-52. https://doi.org/10.1049/ic.2012.0063

Analytical Solution for Switched Band Matching Networks

Norouzian, F. and Gardner, P.
School of Electronic, Electrical and Computer Engineering
University of Birmingham
Birmingham, UK
FXN837@bham.ac.uk

***Abstract* — In this paper, an analytical solution is presented for a dual band switched matching network. By means of a detachable stub it provides the required matching impedances for different frequencies. The analytical solution enables an investigation of range of frequencies and impedances achievable. This solution provides values for the lengths of the transmission lines and stubs to give more precise results and shorten the design stage. The solution is tested analytically and shown to work for several different ranges of frequencies and impedances. Based on this solution, an example switched matching network is designed, fabricated and tested. This analytical solution can be applied to the design of switched band matching networks for many applications (e.g. PAs, LNAs, Antennas etc).**

***Keywords* — Analytical model, dual band, impedance matching, Transmission lines**

I. Introduction

The significant increase in demand for wireless communication systems and the proliferation of communication standards has created interest in more efficient ways of sharing the spectrum in the last few years. Software Defined Radio (SDR) provides an adaptable technology with the potential to improve use of spectrum holes efficiently. At RF and microwave component level, one of the resulting challenges is the design of multiband matching networks (MN). In [1], a technique for dual band MN was introduced using an output-matching to provide first frequency and a shunted switchable stub to produce second frequency. The same technique was used in [2] and [3] with additional stubs to provide three bands of operation. In [4] and [5], the designers tried to make the transmission line shorter and compact the circuits even more. This aim was achieved by implementing a reconfigurable stub for the first matching network consisting of two stubs and a transmission line between them, and a series of transmission lines with switches. However there is a trade off between compactness and extra insertion loss in the MN due to number of switches.

The MNs mentioned above provide a promising approach for multiband problems, but there are issues about the achievable frequency ranges. To address this

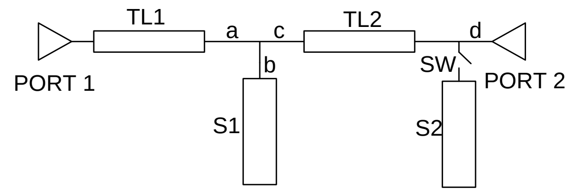

Fig. 1. Detached stub matching network

issue, an analytical solution is required. Furthermore, such a solution will help circuit designers to arrive at optimum multiband MNs in a shorter time.

The present paper is divided into three sections. Equations to design dual band MN are proposed in section II, followed by numerical examples and performance obtained by simulation in the next section. An experimental example based on the derived analytical solution, is discussed in section IV along with measurement results.

II. Analytical Solution

The employed MN is based on the concept which is used in [1]. The first stub is fixed and the second one is connected by a switch. With the switch OFF, the MN provides a required impedance at the first required frequency (f_1) and in ON state of the switch, the desired impedance at the second frequency (f_2) is met.

The analytical solution is derived from MN shown in Fig. 1. The equations are derived for ideal and physical transmission lines with effective dielectric constant (ε_r).

A. Ideal Transmission line

The ideal transmission line is utilised to prove the possibility of using analytical solution. The whole idea of this method is to match by aid of a designated transmission line and a stub for each frequency. The transmission line TL1 of length l provides $Y_0 + jB$ at point a and jB is eliminated by introducing the susceptance of an open stub, equal to $-jB$ by S1. The required impedance looking into TL1 at port 1 at the first frequency is $Z_{L1}$and defined as $R_{L1} + jX_{L1}$. At point a, admittance (Y_1) can be written as:

$$Y_1 = Y_0 \frac{Z_0 - X_{L1} \tan \theta_{L1} + jR_{L1} \tan \theta_{L1}}{R_{L1} + j(X_{L1} + Z_0 \tan \theta_{L1})} \quad (1)$$

where $Z_0$and $\theta_{L1}$are the characteristic impedance and the electrical length of TL1, respectively.

Splitting Y_1 into real part and imaginary part yields (2) and (3) respectively.

$$Re(Y_1) = \frac{R_{L1}(1 + \tan^2 \theta_{L1})}{R_{L1}^2 + (-X_{L1} + Z_0 tan\theta_{L1})^2} \quad (2)$$

$$Im(Y_1) = \frac{R_{L1}^2 tan\theta_{L1} - (Z_0 + X_{L1} tan\theta_{L1})(-X_{L1} + Z_0 tan\theta_{L1})}{Z_0[R_{L1}^2 + (-X_{L1} + Z_0 tan\theta_{L1})^2]} \quad (3)$$

Given that the real part of Y_1 is equal to the characteristic admittance of the system, Y_0, the electrical length of the transmission line can be obtained by the following equation.

$$\theta_{L1} = \tan^{-1}\left(\frac{-X_{L1} - \sqrt{R_{L1}[(Z_0 - R_{L1})^2 + X_{L1}^2]/Z_0}}{R_{L1} - Z_0}\right) \quad (4)$$

By substituting θ_{L1}value back into (3), the susceptance part of Y_1, B, can be obtained. The value of B can be eliminated by the open stub S1. The admittance at b in Fig. 1 is $jY_0 tan\theta_{S1}$ and should be equal to $-jB$. So the electrical length of the stub can be calculated by

$$\theta_{S1} = -\tan^{-1}(\frac{B}{Y_0}) \quad (5)$$

To provide the desired impedance $Z_{L2} = R_{L2} + jX_{L2}$ at f_2 , the second stub is introduced into the circuit by turning the switch ON. To calculate the length of the second transmission line and stub (TL2 and S2 respectively), the admittance at c (Y_3) is calculated by (6).

$$Y_3 = \frac{Z_0 + X_{L2} \tan(\theta'_{L1}) + jR_{L2} \tan(\theta'_{L1})}{R_{L2} + j(Z_0 \tan(\theta'_{L1}) - X_{L2})} + j\,Y_0 \tan(\theta'_{s1}) \quad (6)$$

The physical length of TL_1 and S_1 are fixed but their electrical lengths vary as the frequency changes; therefore, $\theta'_{L1}$and $\theta'_{s1}$are introduced which are electrical length of first transmission line and stub at f_2, respectively. Following the same procedure by applying $1/Y_3$ instead of Z_{L1}^*, we can calculate the electrical lengths of $TL_2$and S_2.

The derived analytical solution is applicable for multiband MNs. This can be done by adding additional switched stubs, position relative to S_1, by repeated application of (6) and back to (3)-(5).

B. Physical Transmission line

For practical applications, the above introduced algorithm needs to be implemented in a physical transmission line medium such as microstrip. To find the lengths of transmission lines in microstrip, the physical lengths need to be divided by $\sqrt{\varepsilon_e}$ yielding (7) where ε_e denotes effective dielectric constant.

$$l = \frac{\theta . c}{\sqrt{\varepsilon_e} 2\pi f} \quad (7)$$

III. Numerical Examples

To verify the presented approach, the equations have been applied to several different numerical values in different ranges of frequencies and one of them is presented in this section. A Gallium Nitride (GaN) HEMT from Nitronex is chosen as an example. Two different frequencies are selected and appropriate impedances are obtained from load pull information in the device datasheet. The required impedances are $0.49 + j0.366$ and $1.052 + j0.456$ at 1800 and 900 MHz, respectively. The MN has been designed so that the required impedance for the higher frequency is provided by the OFF state of the switch, since the amount of loss in switch in its ON state increases at higher frequency. Similar to previous section, appropriate lengths for the transmission lines and stubs are calculated in two different versions, ideal and physical transmission lines.

A. Ideal Transmission line

Using (3-5) the value of B, $\theta_{L1}$and $\theta_{S1}$are calculated respectively. In next step Y_3 is obtained using (6). Using the same procedure θ_{L2} and θ_{S2} are calculated. These results are used in the simulations and the simulation outputs are shown Fig. 2 (a), confirming good agreement with the required impedances taken from the device datasheet.

In the first frequency, one transmission line and one stub is used to match to the required impedance. The second desired impedance is converted to Y_3 at point c in

Fig. 1. The second line and stub parameters are calculated to transform Y_3 at the second frequency to Y_0 at points c and d, respectively. No further iteration of the first line and stub are required to achieve this. The presented method proves that there is no forbidden region to match any dual frequencies by this MN, because whatever the value of Y_3, it can, in principle, be matched using a single line and stub.

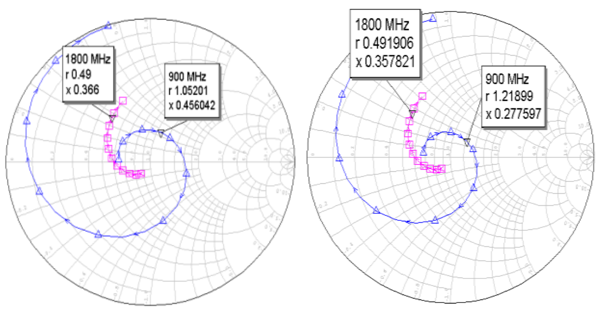

(a) (b)

Fig. 2. Simulation result (a) ideal transmission line (b) physical transmission line

B. Physical Transmission line

The electrical lengths of the transmission lines in this case are evaluated as before and their physical lengths are found by use of (7). Fig. 2(b) shows the simulation results based on the calculated lengths.

The results show a perfect match at 1800MHz and a reasonably close match at 900MHz. The reason for the difference observed in second frequency is the discontinuity of the T-junction. One solution to resolve this issue is to optimize the MN to compensate the discontinuity effect of the T-junction. Taking into account the discontinuity and fine tuning the simulation will give the result presented in Fig. 3 that shows good agreement at 900 MHz.

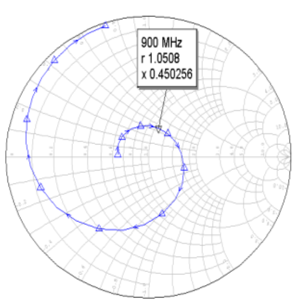

Fig. 3. Simulation result after adjustments

VI. EXPERIMENTAL

The MN based on the calculation in the last part was built, to prove the validation of the algorithm. It was fabricated on microstrip substrate of thickness of 0.76 mm and relative dielectric constant of 3.5. A PIN diode was used as the switch because of its advantages such as low insertion loss, high isolation, high switching speed and excellent power handling at microwave frequencies [6]. The PIN diode was type BAR50 from Infineon.

The simulation and measurement results are compared and plotted by their magnitude (Fig. 4) and on the Smith Chart (Fig. 5). The markers on Fig. 5 ((a) and (b)) indicate the reflection coefficient at the intended frequencies for the ON and OFF state (1800 and 900 MHZ, respectively). Both graphs are shown good agreement between simulation and measurement. The small differences are due to real components and their tolerances.

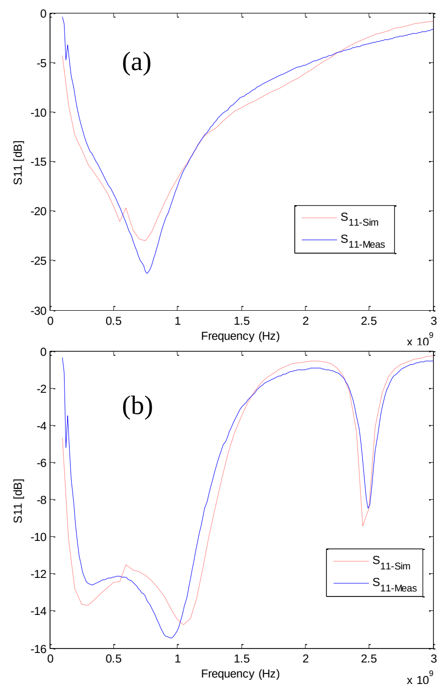

Fig. 4. Simulated and measured S11 in (a) OFF and (b) ON state

V. CONCLUSION

In this contribution, for the first time, the feasibility of multiband MNs for different frequencies, by aid of derived equation, has been shown. The proposed theoretical approach, based on the detached stub MN, provides a closed-form and recursive solution to design dual-band MNs precisely, given any two frequencies. Furthermore this method can be applied not only for two

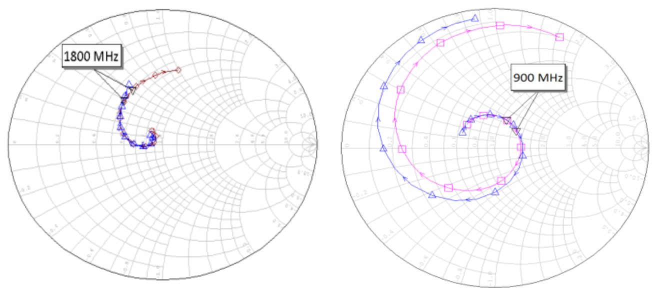

(a) (b)

Fig. 5. Simulated and measured input impedance of MN (a) OFF state and (b) On state

but for several band MNs. Numerical and experimental results have been presented by this work and the results were compared to prove the validity of the algorithm. The presented MNs and derived algorithm could be applied to a wide range of multiband components, such as antennas, LNAs and PAs. These promising results encourage further research on designing multiband MNs that take account of harmonic termination requirements, which are important in power amplifier applications. Investigation of nonlinearity caused by a PIN diode is also a matter of interest.

VI. REFERENCE

[1] A. Fukuda, H. Okazaki, T. Hirota and Y. Yamao, “Novel 900 MHz/1.9 GHz Dual-Mode Power Amplifier Employing MEMS Switches for Optimum Matching”, *IEEE Microwave and Wireless Components Letters,* vol.14, no.3, pp. 121-123, March 2004.

[2] A. Fukuda, H. Okazaki, S. Narahashi, T. Hirota and Y. Yamao, “A 900/1500/200-MHz Triple-Band Reconfigurable Power Amplifier Employing RF-MEMS Switches”, *IEEE,* pp. 657-660, 2005.

[3] H. M. Nemati, J. Grahn and C. Fager, “Band-Reconfigurable LDMOS Power Amplifier”, in *40th European Microwave Conference,* 2010, pp.978-981.

[4] A. Fukuda, H. Okazaki and S. Narahashi, “A Novel Compact Reconfigurable Quad-band Power Amplifir Employing RF-MEMS switches”, in *36th European Microwave Conference,* 2006, pp. 344-346.

[5] A. Fukuda, T. Furuta, H. Okazaki, S. Narahashi, “A 0.9-5-GHz Wide-Range 1 W-Class Reconfigurable Power Amplifier Employing RF-MEMS Switches”, *IEEE,* pp. 1859-1862, 2006.

[6] M. Watertown, *The PIN Diode Circuit Designers’ Handbook,* Massachusetts: Microsemi Corporation, 1998.